(Received 24 January 2025, Accepted 31 March 2025, Scheduled 14 April 2025)

Multi-Layer Square Coil-Based Wireless Power Transfer for Biomedical Implants

Hala K. Abduljaleel[1, 3, *], Sadik Kamel Gharghan[2], and Ahmed Jamal Abdullah Al-Gburi[4, *]

[1] *Electrical Engineering Dept., University of Technology-Iraq, Alsina'a Street, Baghdad 10066, Iraq*
[2] *Electrical Engineering Technical College, Middle Technical University-Baghdad, Iraq*
[3] *College of Engineering, Al-Iraqia University, Saba'a Abkar Compex, Baghdad, Iraq*
[4] *Center for Telecommunication Research & Innovation (CeTRI)*
Fakulti Teknologi Dan Kejuruteraan Elektronik Dan Komputer (FTKEK)
Universiti Teknikal Malaysia Melaka (UTeM), Jalan Hang Tuah Jaya, 76100, Durian Tunggal, Melaka, Malaysia

ABSTRACT: Biomedical devices (BDs) monitor vital signs and diagnose illnesses to improve patients' lives. These BDs rely on battery power, which is often short-lasting. To address this limitation, wireless power transfer (WPT) has been proposed in research as a solution for wirelessly recharging BD batteries. This paper aims to enhance WPT in a non-radiative near-field system for implanted BDs by designing and fabricating a triple-layer receiver coil operating in the 13.56 MHz ISM band. First, three square coil models — single-layer, double-layer, and triple-layer — were developed and simulated using HFSS ANSYS software. The coil models were tested at air gaps ranging from 2 to 40 mm between the transmitter and receiver coils. The single-layer and double-layer coils, each with a receiver coil size of $10 \times 10 \times 0.5$ mm, achieved transfer efficiencies of 76.19% and 80.03%, respectively, at an air gap of 10 mm. In contrast, the triple-layer coil, designed with a receiver coil size of $10 \times 10 \times 1.5$ mm, attained a transfer efficiency of 87.83% at the same air gap. Additionally, the study analyzed the specific absorption rate (SAR), which was measured at 0.1823 W/kg for 1 g of tissue. Second, the triple-layer square coil was validated through fabrication and experimental testing in different environments, including air, acrylic, and biological tissue (beef). The results demonstrated transfer efficiencies of 80%, 77%, and 63% in air, acrylic, and tissue, respectively. Moreover, the experimental results closely matched the simulation ones, confirming that the triple-layer square coil model accurately represents real-world performance.

1. INTRODUCTION

Wireless power transfer (WPT) technology has become a vital solution for implantable medical devices such as pacemakers and neurostimulators, offering a reliable and contactless power delivery method while eliminating the need for physical connectors [1, 2]. Inductive coupling techniques are widely employed to enhance power transfer efficiency without compromising patient safety [3]. Optimizing coil placement and maintaining appropriate spatial separation between the transmitter and receiver improve performance [4]. Electromagnetic waves, particularly those at lower frequencies like microwaves and radio waves, play a crucial role in medical applications due to their ability to penetrate biological tissues [5]. This characteristic makes them suitable for diagnostic imaging, treatment procedures, and wireless medical communication within the Industrial, Scientific, and Medical (ISM) band [6]. Utilizing this frequency range enables cost-effective remote monitoring and control of medical devices. Still, it is essential to adhere to strict safety and security protocols to prevent interference and ensure compliance with US Food and Drug Administration (FDA) and European Medicines Agency (EMA) regulations [7, 8].

A critical aspect of WPT systems is the design and fabrication of the receiver coil, which significantly influences both efficiency and practicality in implantation [8]. Printed circuit boards (PCBs) play a fundamental role in electronic circuits, providing both mechanical support and electrical interconnection for components. Modern PCBs, manufactured using surface-mount and through-hole techniques, are commonly constructed from FR4-based glass fiber composites due to their durability and high specific strength. Copper, a key conductive material, enhances PCB performance with its excellent electrical conductivity, corrosion resistance, and thermal stability.

By integrating advancements in PCB technology with an optimized system utilizing graphene nanocomposites [9, 10], this research aims to reduce the size of implanted receiver coils while improving power transfer efficiency. Achieving this balance will contribute to the development of more compact, efficient, and safer implantable medical devices, ultimately enhancing patient outcomes and quality of life.

This research aims to reduce the dimensions of implanted receiver coils while enhancing power transfer efficiency. Previous studies [11, 12] achieved good efficiency using an implanted coil with a 20 mm diameter. However, the current research demonstrates even greater efficiency by utilizing a three-layer receiver coil (TLRC) and reducing the implanted coil size to 10 mm.

* Corresponding authors: Ahmed Jamal Abdullah Al-Gburi (ahmedjamal@ieee.org); Hala Kamal Abduljaleel (hala.k.abdaljleel@aliraqia.edu.iq).

This work advances wireless power transmission (WPT) for biomedical implants by integrating several key innovations that enhance efficiency and ensure safety. It introduces a novel approach to improving WPT for implantable medical devices by significantly reducing the receiver coil size while maintaining high efficiency. The proposed TLRC, with a compact 10 mm size, is fabricated using a PCB to ensure practical applicability. The system was extensively tested under realistic conditions, including biological tissues, to validate its performance.

Beyond the technical advancements, this study benchmarks the proposed system against existing WPT designs, demonstrating an impressive 87.9% transfer efficiency — outperforming previous methods. The effectiveness of the TLRC system was confirmed through real-world implementation and comparisons with prior studies, highlighting its superior efficiency and potential for next-generation biomedical implants. These contributions collectively advance the development of safer, more efficient, and miniaturized implantable medical devices, addressing critical challenges in wireless power transfer technology.

2. RELATED WORKS

Previous research has explored realistic and cost-effective approaches to developing WPT systems that meet both current and future demands. Mahmood et al. [13] proposed a WPT method that reduces power consumption, thereby extending the lifespan of biomedical sensors (BMSs) and biomedical devices (BMDs). Their system utilizes a magnetic resonance WPT setup with a spider coil to power the proposed BMD. The transmitter and receiver coils are separated by 60 mm, operating at a frequency of 2.4 GHz and delivering a voltage of 5 V.

When being tested at voltages of 5, 10, 15, 19, 23, and 25 V, the system achieved efficiencies of 73.68%, 17.40%, 8.81%, 5.49%, 4.08%, and 3.19%, respectively, at a 10-mm air gap. This study focused on miniaturizing the transmitter and receiver coils, a crucial factor for implanted devices.

Kamarudin et al. [14] introduced a highly coupled magnetic resonance coupling (MRC) method for WPT, optimized for 5G frequencies and specifically designed for near-field electromagnetic energy transfer. This technology enables efficient power transmission in compact, internet of things (IoT)-enabled electronic devices. The MRC WPT designs were optimized using the full-wave electromagnetic simulator CST Microwave Studio, and closed-loop equations were formulated to evaluate the efficiency of 5G MRC WPT. A circular antenna achieved the highest efficiency of 31.58% at a 2-mm distance, followed by 31.26% at 3 mm and 31.02% at 4 mm. Additionally, the circular MRC design improved efficiency by 25% compared to the square-shaped design.

In contrast, the current research employs a square-shaped double-layer coil, which further enhances efficiency. Luo et al. [11] presented a design and optimization technique for wireless power transmission in implanted brain recording microsystems using inductive coupling coils. The method's goal is to optimize power transfer efficiency, minimize externally transmitted power, and guarantee the safety of biological tissue. Planar spiral coils are created explicitly for brain recording implants because of size constraints, transmission high-power needs, and bio-compatibility. The design functions at a frequency of 13.56 MHz, achieving a power transfer efficiency of 70%, near the theoretical maximum of 71.9%. Ahire et al. [15] utilized square-shaped printed spiral coils (PSCs) as both the primary and secondary coils to investigate the feasibility of wirelessly recharging the battery of a biologically implanted pacemaker. The square-shaped PSCs' geometrical characteristics are optimized utilizing the Finite Element Method (FEM) simulation technique. The receiving coil is enclosed inside the implant. MRC tests are performed at frequencies between 300 kHz and 800 kHz as well as 6.78 MHz and 13.56 MHz. Analytical and modeling approaches provide better efficiency at a frequency of 6.7 MHz, yielding 85.51% efficiency with a 100 Ω load. The voltage gain achieved by the physical technique closely matches the analytical and simulation methods. This research conducted experiments using various loads to assess the stability and dependability of the system under varied load conditions.

Mahmood et al. [16] analyzed the transfer efficiencies and powers for a 50 Ω resistive load with four layout designs: spider-spider, spiral-spiral, spiral-spider, and spider-spiral. The study revealed a transfer efficiency of 31.11% and an output power of 6.88 W with a 4 cm air gap and 20.02% transfer efficiency and 1.71 W output power with a 70 mm distance air gap. With a 12-cm air gap between the transmitter and receiver coils, the efficiency and output power decreased to 2.09% and 0.207 W, respectively. The spiral-spider topology exhibited a reduction in power and efficiency below 0.189 W and 0.52% when the air gap was increased to 15 cm. The spiral-spider architecture demonstrated superior transfer efficiency and output power performance compared to other topologies. The research emphasizes the significance of using air gaps in constructing efficient transmitter and receiver coils. Zhao and Mai [17] introduced a five-coil group integrated for implanted wireless devices. The construction comprises radiating and driving coils, both resonating at 13.56 MHz. This creates an even magnetic distribution, enhancing resistance to dislocations. S parameter determines the system's effectiveness at a frequency of 13.56 MHz. The structure is dense and appropriate for implants. The experimental findings indicate that the efficiency may achieve 54.7% when coils are aligned and remain almost constant, notwithstanding any dislocation. Several efficiency values exceed 50%, which ensures effective and consistent power transmission. Wang et al. [18] proposed near-field WPT technology to provide implantable devices. The WPT system operates at a 403 MHz band. It consists of an external transmitter and an inside receiver with a single-turn loop. They recorded a Power Transfer Efficiency (PTE) of 57.9% across a 6 mm distance, with 1 mm passing through the air and human tissue with a thickness of 5 mm. The input power is 159 mW with a rectifier circuit to transfer 403 MHz of the signals into DC for a 1.5 kΩ load, with a 73.2% measured efficiency. The calculated overall PTE of the suggested WPT system is 42.4%.

Xu et al. [12] presented an improved implanted wireless power transmission mechanism. A dual-coil model was developed, and the parameters influencing transmission efficiency were analyzed. The impact of coil structure was examined using HFSS (High-Frequency Structure Simulator) simulations,

and the optimal coil parameters were verified. The system connection was successfully established, and the measurements demonstrated the correlation between load and output power. The input and output powers were 200 mW and 70 mW, respectively, at a transmission distance of 6 mm, a frequency of 13.56 MHz, and an impedance of 1 kΩ. The system's transmission efficiency was improved by 35%.

Bao et al. [19] proposed a method for enhancing the coupling coefficient (k) of an inductive link in a WPT system for implanted devices. The transmitter coil was designed as a spiral shape with a radius of 20 mm, while the receiver coil was a solenoid with a wire pitch of 0.7 mm. The syste's coupling coefficient (k), power transfer efficiency (PTE), and maximum power delivered to the load (MPDL) were determined through simulation and experimentation. Various mediums, including air, muscle, and bone, were tested to evaluate their impact on the transmission and reception coils. In muscle and bone mediums, the PTE was 44.14% and 43.07%, respectively, while the MPDL was 145.38 mW and 128.13 mW.

Abed et al. [20] conducted an advanced mathematical and theoretical analysis to enhance the efficiency of inductive coupling. This was achieved using high-efficiency Class-E amplifiers with optimal input impedance at a frequency of 13.56 MHz. The resistance of the implanted device ranged from 200 Ω to 500 Ω, with increments of 50 Ω. The power amplifiers exhibited an efficiency of 45% with a load resistance of 50 Ω. This efficiency increased to 49% when the load was adjusted to 41.89 Ω, with a coupling coefficient of 0.087.

Ouacha et al. [21] introduced a novel method to enhance wireless energy transfer using the differential evolution algorithm (DEA) to improve PTE and power delivered to the load (PDL). The proposed approach was validated by comparing results with existing methods, achieving a PTE of 95% and delivering 136 mW of power to the load at a distance of 130 mm. The metaheuristic method significantly improved WPT performance, leading to a 95% PTE and a power output of 136 mW to the load.

The researchers mentioned above developed a WPT system with a considerable transfer distance. However, the present study focuses on increasing the efficiency of the wireless power transmission system by optimizing the design of the transmitting and receiving coils. To achieve this, the study emphasizes increasing the number of layers in the receiving coil while reducing its size to enhance power transmission efficiency while ensuring patient comfort. Furthermore, various experimental tests were conducted on the manufactured coils in environments that simulate real-life conditions, including air and biological tissues such as beef. These tests provided a more accurate understanding of the system's performance in real-world scenarios, improving the reliability and applicability of the findings. Additionally, the specific absorption rate (SAR) was measured to ensure the system's safety and compliance with international health standards regarding the exposure to electromagnetic radiation.

This study employs a transmitter coil with a triple-Rx square spiral coil to describe a wireless power transmission system for implanted biomedical devices. The receiver's outer diameter is 10 mm, while the transmitter's outer diameter is 32 mm. Printed on an FR4 substrate, the system achieves a coupling distance of 2–40 mm within the ISM band at a frequency of 13.56 MHz.

3. MATERIALS AND METHODS

This part introduces and examines the inductive coupling technique based on WPT, TLRC theoretical model, TLRC analytical models, and the simulation implemented using HFSS software.

3.1. TLRC-Based Inductive Coupling Method

Figure 1 illustrates that the WPT technique consists of three primary components: the primary coil (transmitter circuit, Tx), the secondary coil (receiver circuit, Rx), and the load. Generally, a wireless power system comprises a transmitter unit and one or more receiver units [22]. The transmitter unit is connected to the power source (input voltage and oscillator) and converts electricity into an oscillating electromagnetic field, which is achieved through the transmitter circuit [23]. Resonators with a source and receiver coil operating at the same frequency enable magnetic coupling between the two systems, enhancing energy transfer efficiency [24]. If the transmitter and receiver coils resonate at the same frequency, power transmission can occur without requiring a physical connection, such as metal or another conductive material [25].

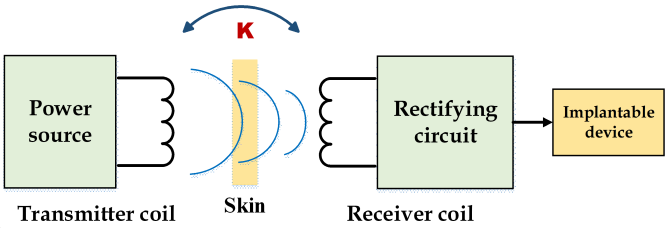

FIGURE 1. Simplified TLRC system.

The receiver captures the energy and converts it back into AC or DC electric current for the use by an electrical load [26]. The coupling device transforms electromagnetic radiation into an electrical current at the receiver [27]. The TLRC approach is the most commonly used and preferred method. This process involves transferring signal power by interconnecting a source that generates magnetic field signals. The primary coil, typically positioned on the exterior of the human body, is used for biomedical applications [28]. According to Faraday's law, voltage is induced in the secondary coil of the receiver, which is often implanted inside the body [29]. While this technology can generate a substantial amount of power, coil alignment is a crucial factor that must be carefully considered [30].

To optimize performance, it is recommended to use a precisely matched coil pair or a well-tuned power supply [31]. The TLRC approach is particularly suitable for transcutaneous applications [32], where WPT occurs between the transmitter and receiver coils. In such applications, the transmitter coils are typically placed on the exterior of the human body, while the receiver coils are positioned internally [33].

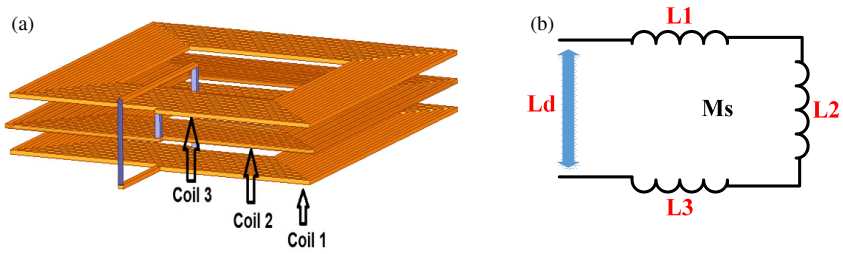

FIGURE 2. (a) Geometrical connection layout of a three-layer spiral coil. (b) Three inductors connected in series.

3.2. TLRC Theoretical Model

The implementation of a particular coil serves three primary purposes: inductance (L), series parasitic resistance (Rs), and parallel parasitic capacitance (Cp) [34]. These parameters are influenced by various geometric factors, including the number of turns (n), track width (w), track spacing (s), inner diameter (Din), and outer diameter ($Dout$) of the copper [35].

The mathematical models describing the square coil are as follows:

The self-inductance of a square coil can be determined using Equation (1) [36]:

$$L = \frac{1.27\mu n^2 d_{avg}}{2}\left[\ln\frac{2.07}{\varphi} + 0.18\varphi + 0.13\varphi^2\right] \quad (1)$$

where μ is the permeability of free space ($4\pi \times 10^{-7}$ H/m); φ is the fill factor; n is the number of coil turns; d_{avg} is the average diameter of the inductor, as in Equations (2), (3), and (4):

$$n = \frac{D_{out}\varphi}{(s+w)(1+\varphi)} \quad (2)$$

$$D_{out} = D_{in} + (2n+1)w + (2n-1)s \quad (3)$$

$$d_{avg} = \frac{(D_{in}+D_{out})}{2} \text{ and } \varphi = \frac{(D_{out}-D_{in})}{(D_{out}+D_{in})} \quad (4)$$

The accuracy of this expression deteriorates as the ratio of s/w increases significantly, particularly when φ is less than 0.1 or n less than or equal to 2. It is important to note that a conventional integrated spiral inductor is designed with a width (s) that is less than or equal to the spacing (w). The spacing between components primarily serves to mitigate the adverse effects of interwinding parasitic capacitance.

The self-inductance of a two-layer or three-layer coil cannot be calculated using Equation (1) because such coils generate mutual inductance between their turns. Instead, the self-inductance is determined using Equation (5) [37].

$$L_d = L_{s1}+L_{s2}+L_{s3}\pm 3M_s \quad (5)$$

Variables L_1, L_2, and L_3 represent the inductance values of the first, second, and third layers. Additionally, M_s denotes the mutual coupling between the three layers, as shown in Figure 2. In the case of a three-layer coil with identical spirals, the self-inductance of each layer can be denoted as $L_1 = L_2 = L_3 = L_s$.

The coupling between the transmitter and receiver coils can be calculated by using Equation (6) [38] as shown below:

$$M = k\sqrt{L_1 L_2} \quad (6)$$

k is an element strongly influenced by the material qualities, the dimensions and shape of the coils, and their relative arrangement with each other. Expressing it analytically with intention is, therefore, a complex procedure. However, Pérez-Nicoli computed it in Equation (7) [39]:

$$k = \frac{r_1^2 r_2^2 \cos\theta}{\sqrt{r_1 r_2}\left(\sqrt{D^2+r_1^2}\right)^3} \quad (7)$$

r_1 and r_2 are the radii of the transmitter and receiver coils; D and θ are the distance and angle between the coils, respectively. However, Equation (7) only applies if $r_1 \leq r_2$.

3.3. TLRC Analytical Models

The TLRC analytical system, incorporating the geometrical parameters of the coil listed in Table 1, was modeled using the ANSYS Electromagnetics Suite 2022 R1 simulator. By utilizing Z-parameters, the electrical characteristics of the coils can be efficiently estimated. These parameters include the inductances of the implanted (receiver) and transmitter coils, coupling and mutual inductance between the coils (k and M), the quality factors of the coils (Q_1 and Q_2), the series resistance of the coils (R_{S1} and R_{S2}), and the maximum transfer efficiency ($\eta_{\max}$). These parameters can be determined using Equations (8)–(13).

$$L_1 = \frac{\mathrm{Im}(Z(1,1))}{2\pi f} \quad \text{and} \quad L_2 = \frac{\mathrm{Im}(Z(2,2))}{2\pi f} \quad (8)$$

$$Q_1 = \frac{\mathrm{Im}(Z(1,1))}{\mathrm{Re}(Z(1,1))} \quad \text{and} \quad Q_2 = \frac{\mathrm{Im}(Z(2,2))}{\mathrm{Re}(Z(2,2))} \quad (9)$$

$$k = \sqrt{\frac{\mathrm{Im}(Z(1,2)) * \mathrm{Im}(Z(2,1))}{(\mathrm{Im}(Z(2,2)) * \mathrm{Im}(Z(1,1)))}} \quad (10)$$

$$R_{S1} = \mathrm{Re}(Z(1,1)), \quad R_{S2} = \mathrm{Re}(Z(2,2)) \quad (11)$$

$$M = \frac{\mathrm{Im}(Z(2,1))}{2\pi f} \quad (12)$$

$$\eta_{\max} = \frac{k^2 Q_1 Q_2}{\left(1+\sqrt{1+k^2 Q_1 Q_2}\right)^2} \quad (13)$$

TABLE 1. Single, double, and triple layer coil systems parameters.

Parameters	Single-layer Design		Double-layer Design		Triple-layer Design	
	Tx	Rx	Tx	Rx	Tx	Rx
D_{out} (mm)	32	10	32	10	32	10
D_{in} (mm)	7	5	7	5	7	5
w (mm)	0.562	0.165	0.562	0.165	0.562	0.165
s (mm)	0.245	0.140	0.245	0.140	0.245	0.140
n (turns)	16	8	16	8 (for each layer)	16	8 (for each layer)
Operating frequency	13.56 MHz		13.56 MHz		13.56 MHz	
Distance between coils (mm)	10		10		10	
Conductor thickness t_c (mm)	0.07		0.07		0.07	
Substrate thickness t_s (mm)	$t_{s1} = 1, t_{s2} = 0.5$		$t_{s1} = 1, t_{s2} = 0.5$		$t_{s1} = 1, t_{s2} = 1.5$	
Substrate dielectric constant $\in_{rFR4}$	4.4		4.4		4.4	
Type of Via	Through hole via		Through hole via		Blind and buried via	

Parameters Z_{11}, Z_{12}, Z_{21}, and Z_{22} correspond to the impedance values and interconnections between the coil ports. Z-parameters play a crucial role in various aspects, including impedance matching, network analysis, design optimization, simulation, and modeling. These parameters help determine the most suitable impedance design to enhance transfer efficiency.

3.4. Simulation of TLRC System for Implantable Device

3.4.1. Single Layer Design

The proposed system consists of a single-layer transmitter and receiver, as illustrated in Figure 3(a). The key design parameters are listed in Table 1. The resonance frequency of the design is set at 13.56 MHz. The system operates in an inductive coupling configuration, with an outer diameter of 32 mm for the transmitter coil and 10 mm for the receiver coil. The system was tested with an air gap of 10 mm separating the transmitter and receiver coils.

The values of L_1, L_2, and M can be calculated using Equations (8) and (12). The coupling coefficient of the receiver coil is determined using Equation (10), while the maximum power transfer efficiency is calculated using Equation (13).

3.4.2. Double Layer Design

This research aimed to achieve effective wireless charging for an implanted device, such as a cardiac pacemaker, by ensuring suitable power transfer. A double-layer coil was used within an acceptable transfer distance, as shown in Figure 3(b), making it well suited for wirelessly implanted devices. The key performance metrics of the design, including inductance, output power, and transfer efficiency, were evaluated at 13.56 MHz. The air gap distance between the transmitter and receiver coils was set to 10 mm.

The use of a double-layer spiral coil demonstrates a significant increase in inductance, coupling coefficient, and quality factor. The double-layer configuration enhances the conductor width, thereby reducing series resistance. This reduction in resistance subsequently improves the quality factor of the coils. Furthermore, adopting a double-layer design allows for the selection of a more optimal inner diameter. The parameters and geometries of the resulting double-layer spiral coils are presented in Table 1.

3.4.3. Triple-Layer Design

This is the most efficient design selected in this phase of the research. The implanted spiral coil was designed using three series-connected coil layers, each precisely dimensionally symmetrical. All parameters and steps used for the single- and double-layer designs were applied here. However, in this design, the three coil layers are connected in series using two types of vias: blind and buried vias, as shown in Figure 3(c).

These configurations were carefully chosen to maximize transfer efficiency, ensuring optimal power transfer with minimal loss. This approach is intended to enhance efficiency and improve performance in real-life applications. The parameters of the triple-layer coil design are presented in Table 1.

3.5. TLRC Experimental Setup

The transmitter and receiver coils were fabricated using the Printed Circuit Board (PCB) technique. The FR4 (flame-resistant) substrates, composed of glass fabric and flame-resistant epoxy resin, were selected for their low water absorption, strong adhesion to copper foil, effective thermal insulation, and exceptional mechanical strength. The substrate thickness was 1 mm for the transmitter and 1.5 mm for the receiver.

The TLRC system design utilized copper for the coils due to its high electrical and thermal conductivity, ensuring efficient signal transmission and minimal power loss. The track width was 0.562 mm for the transmitter coil and 0.165 mm for the receiver coil, with a copper thickness (tc) of 0.07 mm. The receiver coil was fabricated with a triple-layer structure printed on an FR4 substrate, as shown in Figures 4 and 5.

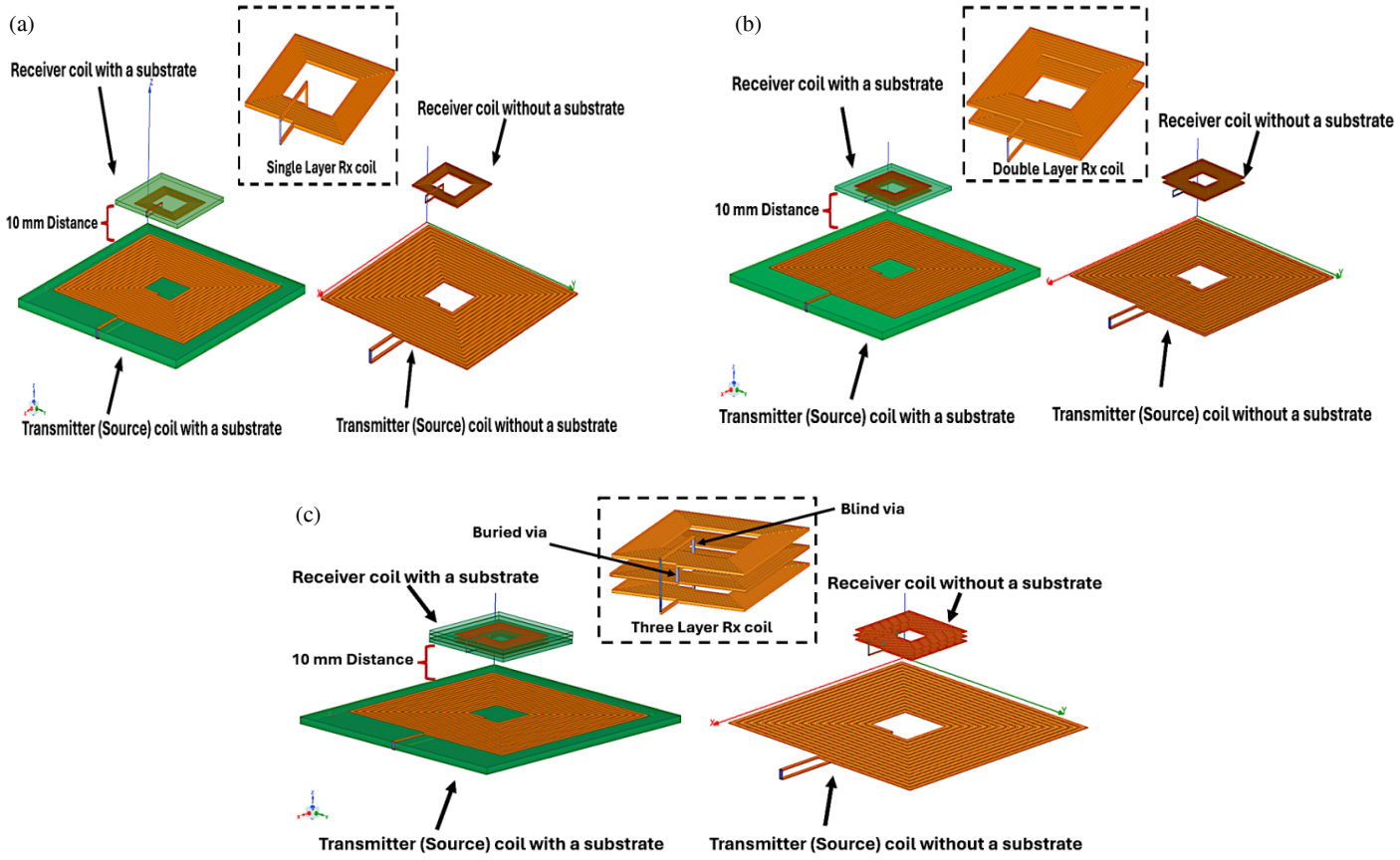

FIGURE 3. TLRC system. (a) Single layer. (b) Double layer, and (c) Triple layer wireless design.

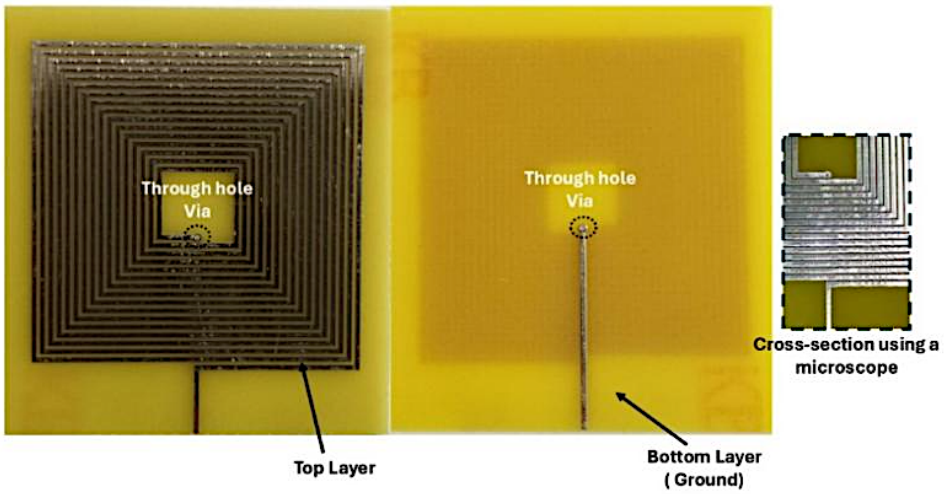

FIGURE 4. The transmitter coil after fabrication.

3.6. SAR Test for Triple-Layer Design

This design simulates how the Specific Absorption Rate (SAR) changes in the human body and head when they are exposed to a magnetic field from a medical wireless system operating in the ISM band (13.56 MHz) with an input power of 1 watt. The human body model was created using ANSYS HFSS to simulate realistic SAR measurements. The receiver coil was placed inside the human body with a 6 mm gap from the transmitter coil, as shown in Figure 6. The SAR distribution inside the head and body was then extracted.

SAR is typically determined as an average over the whole body or a specific amount of tissue, generally 1 g or 10 g. To regulate consumer health and safety, several international agencies mandate that products on the market comply with SAR

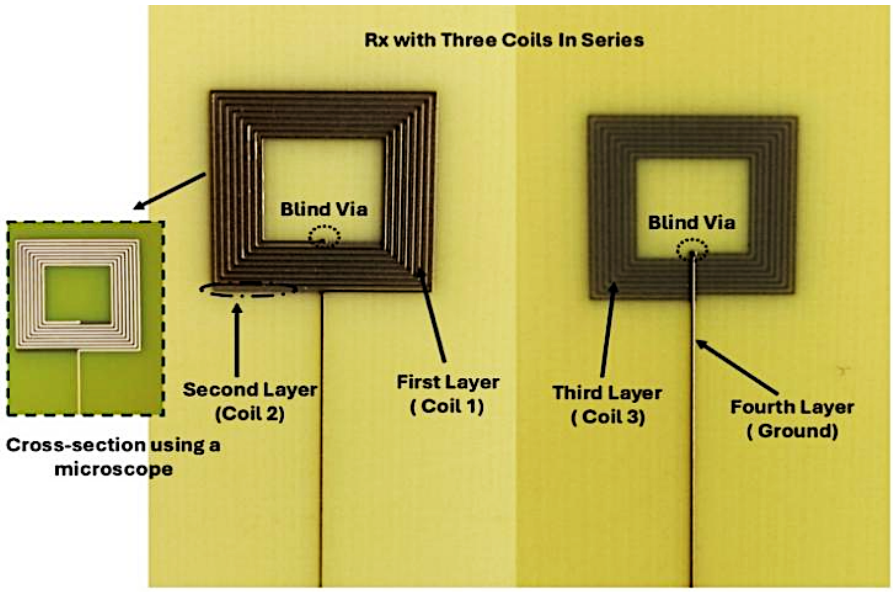

FIGURE 5. Triple-layer receiver coil after fabrication.

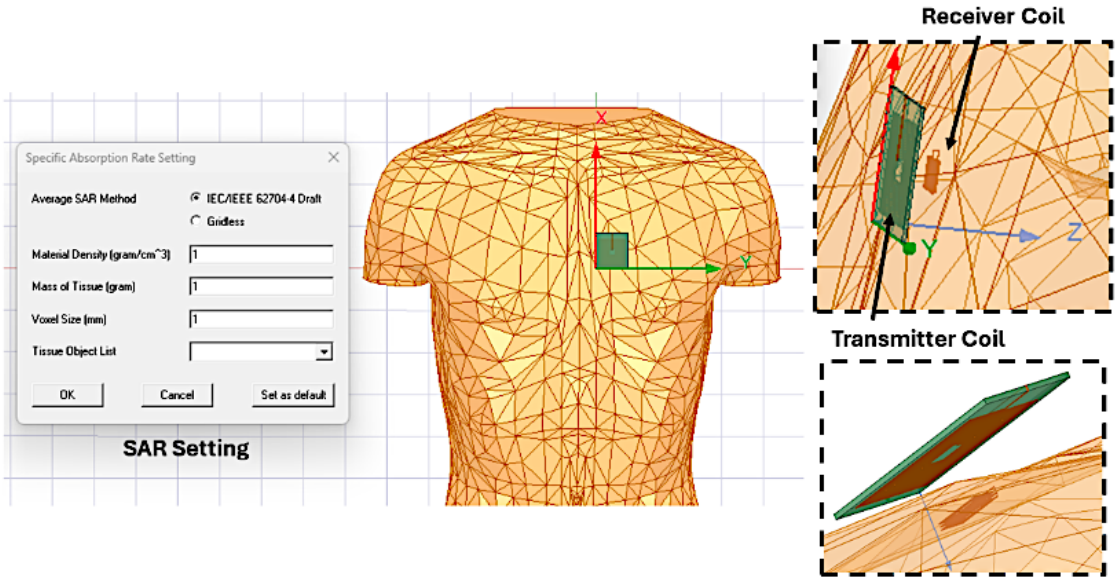

FIGURE 6. Simulation of SAR in wireless power transmission systems for implantable medical devices.

TABLE 2. SAR standards and limits in different regions and countries [40, 41].

Region	SAR Limit
Europe	2.0 W/Kg in 10 g of tissue
Japan	2.0 W/Kg per 10 g of tissue
Australia	2.0 W/Kg per 10 g of tissue
United States and Canada	1.6 W/Kg in 1 g of tissue
Korea	1.6 W/Kg per 1 g of tissue

limitations. The measurement of SAR is becoming increasingly critical for manufacturers of such equipment. The Federal Communications Commission (FCC) of the United States has set the SAR limit for the head at 1.6 W/kg, averaged over a 1 g volume of tissue. In contrast, the European limit is 2 W/kg, averaged over 10 g. The dimensions of the averaging volume significantly influence SAR readings. Table 2 presents the acceptable SAR limits in different regions and countries.

4. RESULTS AND DISCUSSION

4.1. Simulation Result

This section presents the simulation findings for the three spiral coil designs (single-layer, double-layer, and triple-layer) used for wireless power transfer (WPT) at 13.56 MHz. The study

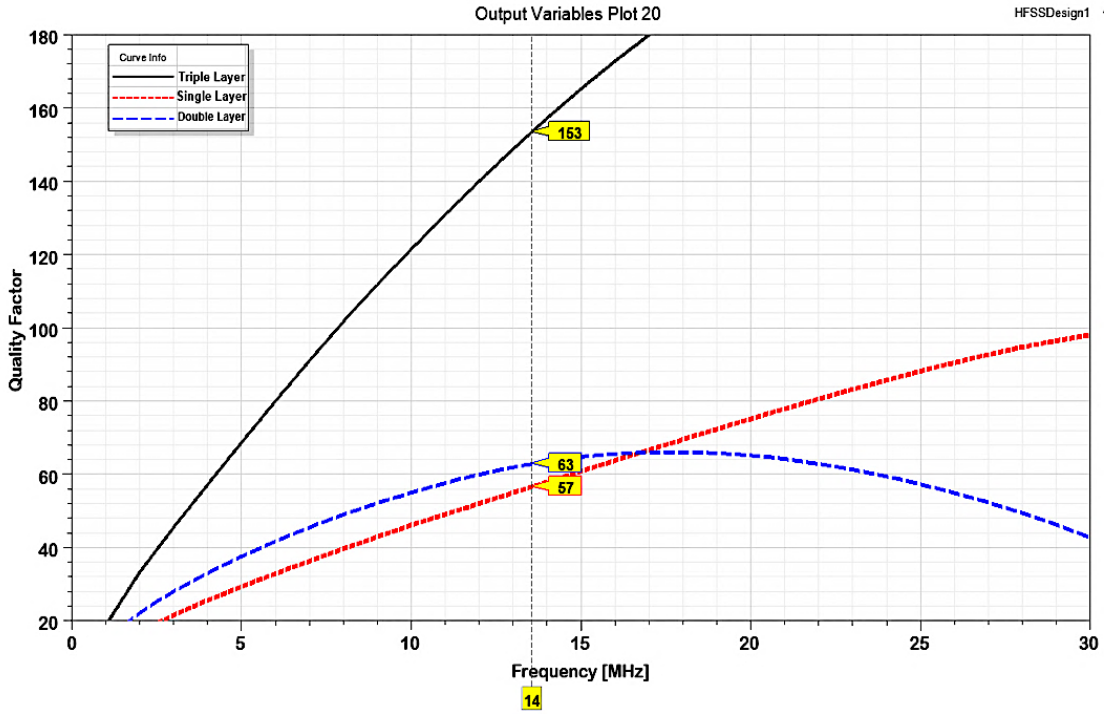

FIGURE 7. Comparison of the quality factor vs frequency for (Single-Double-Triple) receiver coil design at 13.56 MHz.

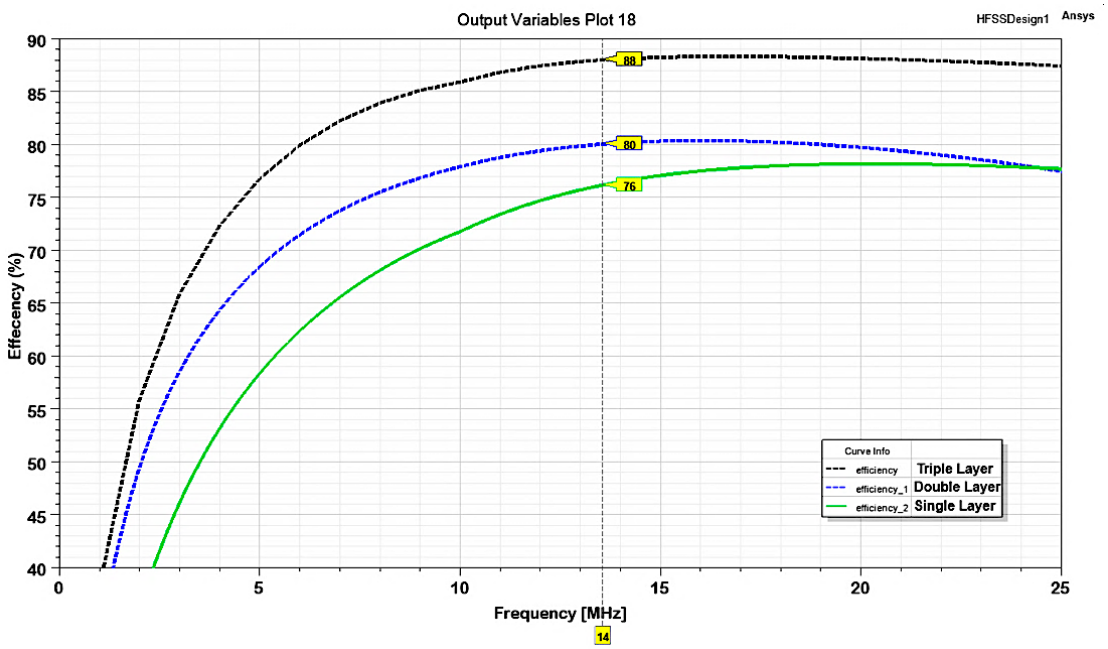

FIGURE 8. Comparison of the efficiency vs frequency for (Single-Double-Triple) Receiver coil design.

analyzes the quality factor values, efficiency versus frequency, and system efficiency across various distances.

4.1.1. Results of Quality Factor and Efficiency of Three Designs

This section compares the three designs to identify the most effective configuration. The quality factor of the receiver coil for each design is shown in Figure 7. The quality factor values were 56.5 for the single-layer design, 62.8 for the double-layer design, and 153.4 for the triple-layer design. Thus, using a triple-layer coil in series significantly increased the inductance of the receiver coil and enhanced the quality factor.

Figure 8 illustrates the efficiency characteristics of the single-layer, double-layer, and triple-layer designs. The triple-layer design achieves a maximum efficiency of 87.97% at the resonant frequency of 13.56 MHz, outperforming the other designs by a substantial margin. In comparison, the

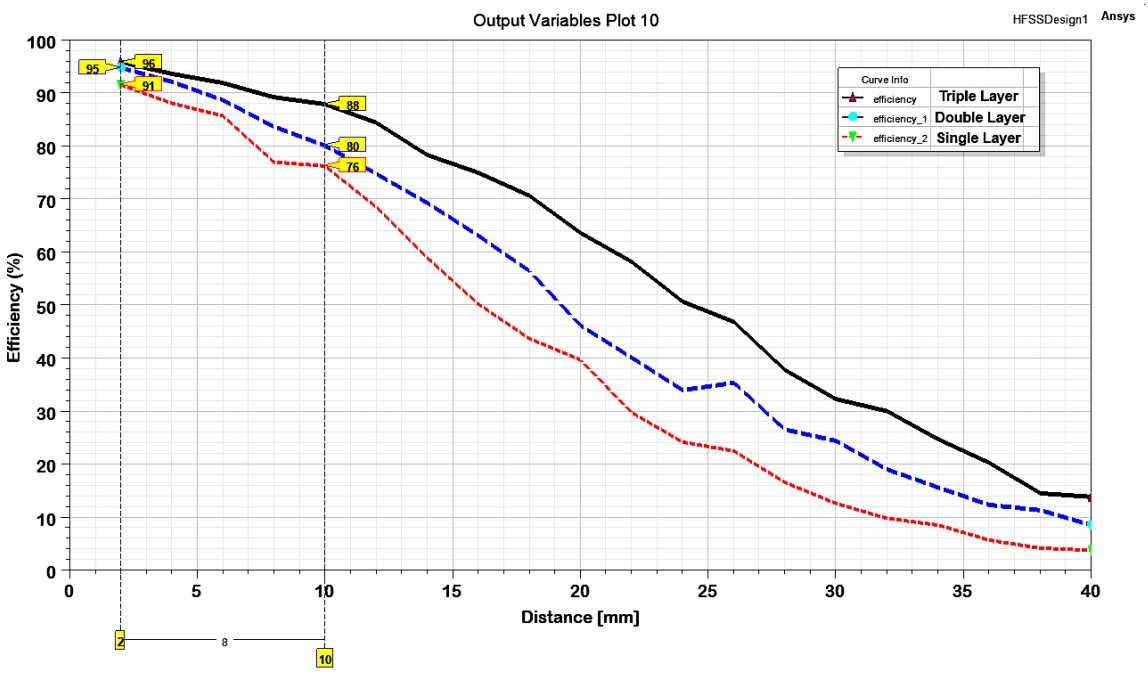

FIGURE 9. Comparison of the efficiency vs distance for (Single-Double-Triple) Receiver coil design at 13.56 MHz frequency.

single-layer design attains an efficiency of 76.16%, while the double-layer design reaches 80.03%. These findings confirm that increasing the number of coil layers improves the overall efficiency of the technology.

Figure 9 illustrates that the triple-layer design achieved a power transfer efficiency of 96% when the transmitter and receiver were positioned 2 mm apart. The efficiency decreased to 88% when the operating distance was increased to 10 mm. The initial design exhibited a decline in transfer efficiency even at the operating distance, while the single- and double-layer designs achieved the desired efficiency at a 2 mm distance. In contrast, their efficiency dropped to 76–80% at the operational distance. Therefore, the triple-layer design proves to be an excellent choice, even when an operating distance of 10 mm is considered.

4.1.2. Result of SAR for Triple Layer Design

The first step in conducting the SAR simulation test was to convert the implanted triple-layer coil into a new model in ANSYS HFSS. The SAR was then tested on a man's left hand. Figure 10 illustrates the SAR distribution for 1 g of tissue in W/kg at a frequency of 13.56 MHz and an input power of 1 W. The highest SAR value recorded during the test was 0.1823 W/kg for 1 g of tissue. The SAR values obtained in the simulation were significantly lower than the limits set by U.S. and European standards for 1 g of tissue.

4.2. Experimental Results

This proposed design was tested at the Ministry of Science and Technology, Department of Industrial Research and Development, and the Electronic Manufacturing Centre. Figure 11 shows that the transmitter and receiver coils were fixed at a 10 mm distance to validate the system design. The Z-parameters of each coil were measured using a Vector Network Analyzer (VNA), with ports 1 and 2 of the VNA connected to the respective coils of the system. This setup allowed for the straightforward extraction of the coils' electrical parameters, as shown in Figure 11.

The mutual inductance was directly obtained by measuring Z_{21} parameter. The Z_{21} parameter was measured by connecting the transmitter coil to port 1 and the receiver coil to port 2 of the VNA at a fixed distance. The impedance of ports 1 and 2, both connected to the VNA, was 50 Ω. The measured mutual inductance between the coils using the VNA was 56.36 nH, while the simulated value was 40.9 nH.

This test determined the coupling ratio between the transmitting and receiving coils and the extent of mutual inductance between them. A high mutual inductance indicated strong coupling between the coils, which is essential for efficient energy transmission applications. Figure 12(a) and Figure 12(b) show the measured electrical parameters of the transmitter and receiver coils, obtained using the VNA device. The mutual inductance value between the two coils was determined from Figure 13.

Subsequently, load resistance was added to the receiver coil, and the resultant output voltage was computed. This method can be used to determine power transfer efficiency. Figure 14(a) illustrates the addition of a 300 Ω load to the receiver coil in the first experiment, where no medium (only air) was present between the transmitter and receiver coils. A Tektronix AFG2021 function generator, capable of generating waveforms with frequencies up to 20 MHz, was used to provide a signal to the transmitter side. A Tektronix digital storage oscilloscope (DSO) recorded and analyzed the output signal from the receiver side, capturing and examining electrical signals. The

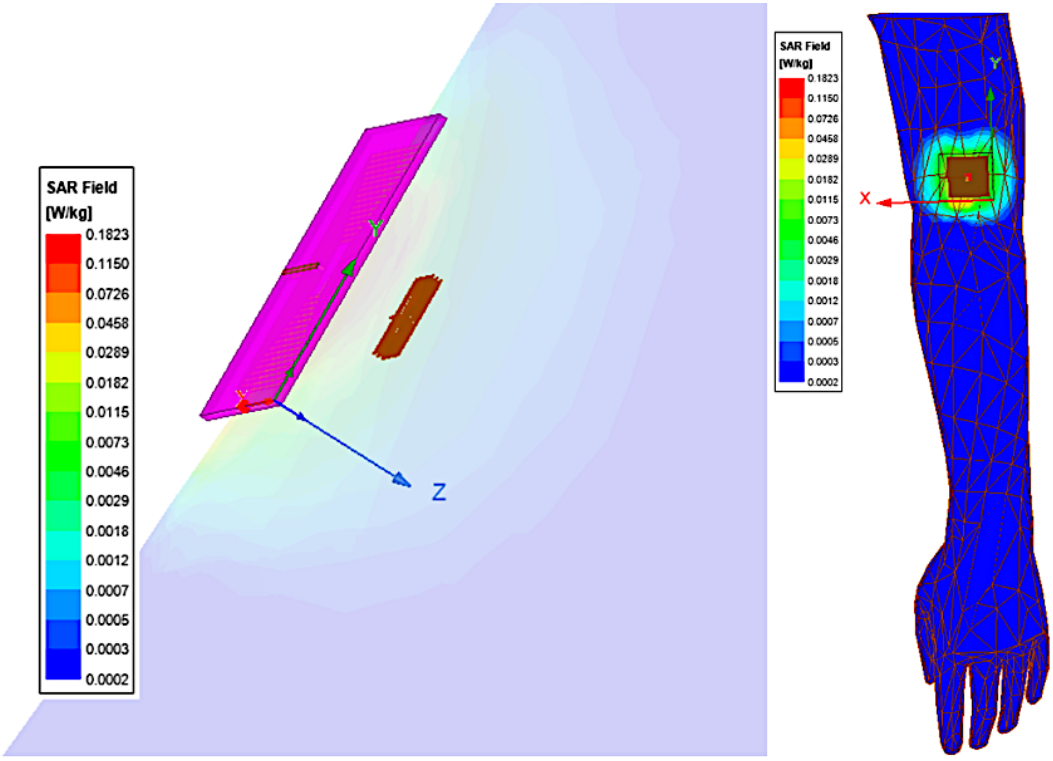

FIGURE 10. SAR simulation test on male left-arm phantom for 1 gram of SAR.

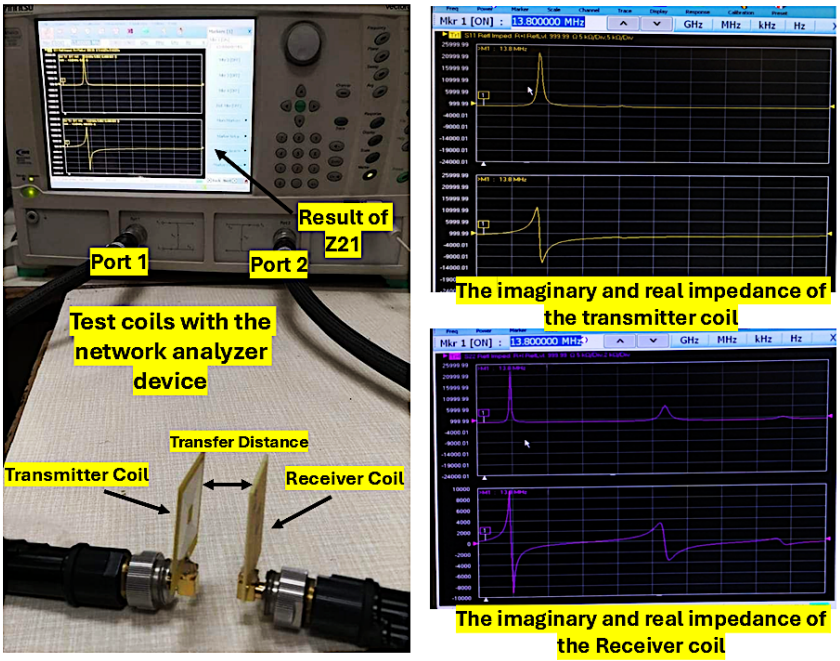

FIGURE 11. Test system setup with vector network analyzer measuring the impedance of transmitter and receiver coils.

displayed waveform was a sine wave, a common periodic signal.

The sine waves exhibited symmetry with respect to the 0 V axis and were pure sine waves without any direct current (DC) offset. The frequency displayed on the screen was 13.5601 MHz. The load resistance influenced signal strength, affecting the power delivered to the load. A lower load impedance increased signal strength by allowing greater current flow, while a higher load impedance reduced signal strength.

Additionally, load resistance affected the waveform shape, with low load impedance resulting in minimal distortions,

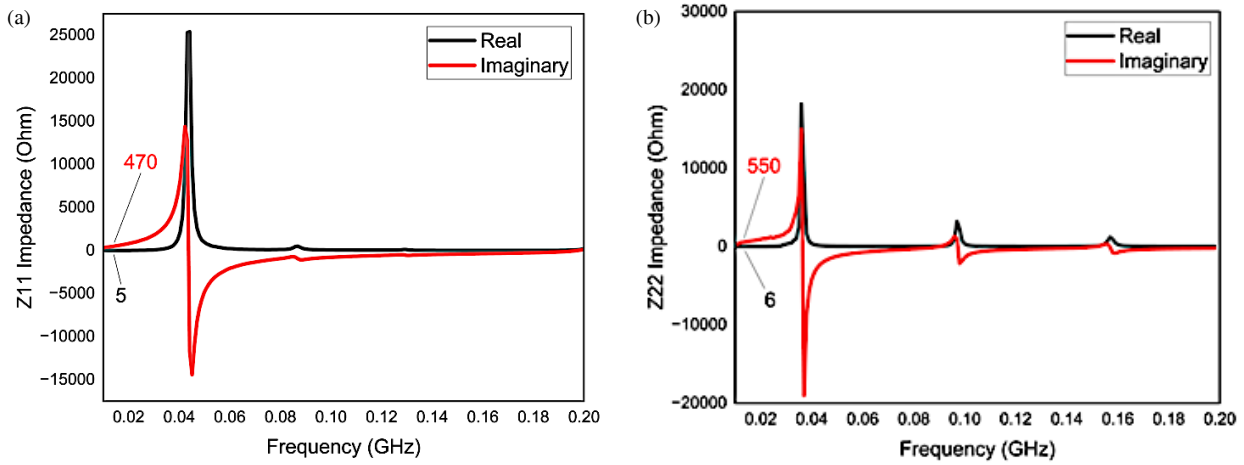

FIGURE 12. The real and imaginary measurement results of (a) the transmitter and (b) the triple-layer receiver coil.

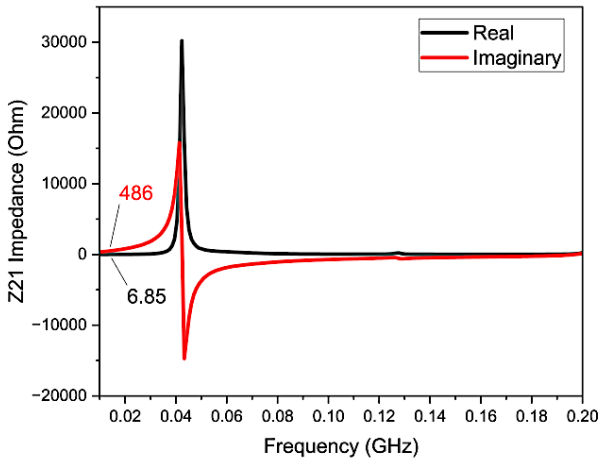

FIGURE 13. The real and imaginary measurements of the reflected impedance Z_{21} for fabricated design.

whereas high load impedance led to significant distortions or timing alterations. The frequency response was also influenced by load impedance, where a high load impedance could cause frequency losses, impacting the system's ability to accurately detect high frequencies. Thus, load resistance played a crucial role in determining signal intensity, waveform integrity, and frequency response.

Furthermore, a second experiment was conducted in which beef tissue was placed between the transmitter and receiver coils, as shown in Figure 15. In a third experiment, the receiver coil was covered with acrylic material to protect it from fluids inside the tissue, ensuring the stability of the test results, as illustrated in Figure 16.

The primary objective of the test was to evaluate the system's performance when it was connected to a real load for practical measurements. This included assessing the system's stability and reliability under different load values, analyzing the impact of the load on the quality and stability of the received signal, and identifying methods to ensure consistent and dependable performance across various load conditions.

The results obtained at a distance of 6 mm showed a 90% efficiency in the air. As indicated in Figure 17, the efficiency decreased to 80% at an operating distance of 10 mm and further dropped to 62% at 20 mm, with a load resistance of 50 Ω. When beef tissue was placed between the two coils at a distance of 6 mm, the measured efficiency was 70%. The efficiency declined to 63% at an operating distance of 10 mm and further to 35% at 20 mm, with a load resistance of 50 Ω. For the receiver coil coated with acrylic material and tested in air, the efficiency at 6 mm was 85%. The efficiency dropped to 77% at an operating distance of 10 mm and 60% at 20 mm, with a load resistance of 50 Ω.

Finally, when the coated receiver coil was placed in beef tissue and tested at a distance of 6 mm, the efficiency was 68%. It decreased to 65% at an operating distance of 10 mm and further to 40% at 20 mm, with a load resistance of 50 Ω. Figure 18 illustrates the impact of various load resistance values on the overall transfer efficiency of the proposed system. At a load resistance of 400 Ω and a distance of 10 mm, the efficiency reached 93% in an air medium. The efficiency decreased to 74% in a beef tissue medium. When the acrylic-coated receiver was tested in air, it achieved an efficiency of 88%. Lastly, when the coated receiver was tested in beef tissue, an efficiency of 73% was obtained..

4.3. Comparison Results with Simulation

Table 3 compares the characteristics of the transmitter and receiver coils obtained from simulation with the experimental results. The measured efficiency was 80%, while the simulated efficiency was 87.9% at a load resistance of 50 Ω and a distance of 10 mm, as shown in Figure 19. The discrepancy in efficiency between the measured and simulated values may be attributed to the precision and quality of the manufacturing technologies used.

Additionally, power losses in the coils occur due to the extra resistance from the SMA ports, welded SMA connections, and vias. Figure 19 illustrates the comparison of transfer efficiency between the simulated and experimental results. Both approaches show a decrease in efficiency as the distance in-

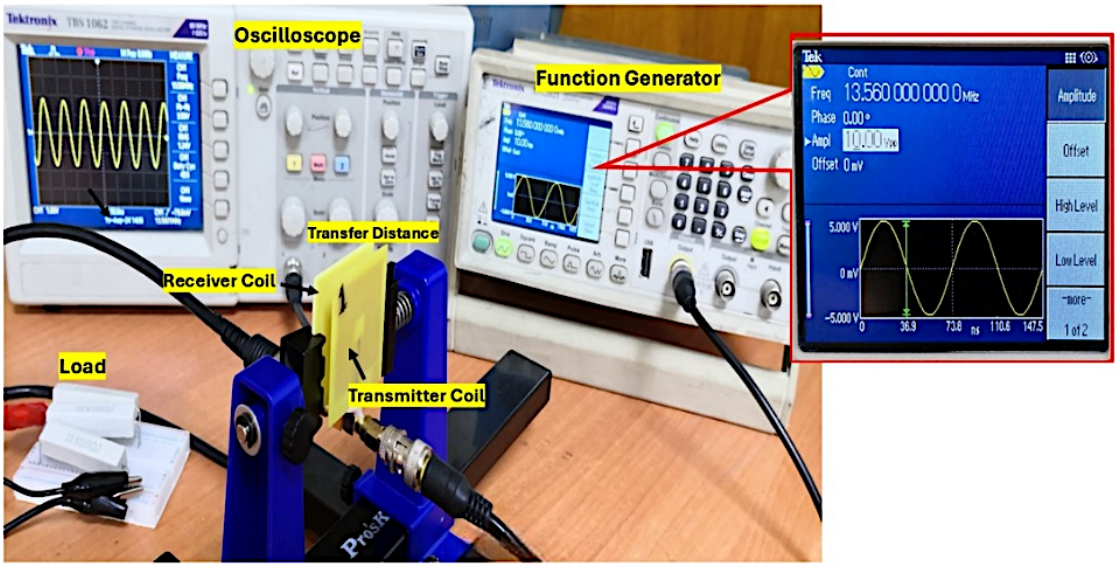

FIGURE 14. System measurement using a load resistor of 300 Ω with air environment.

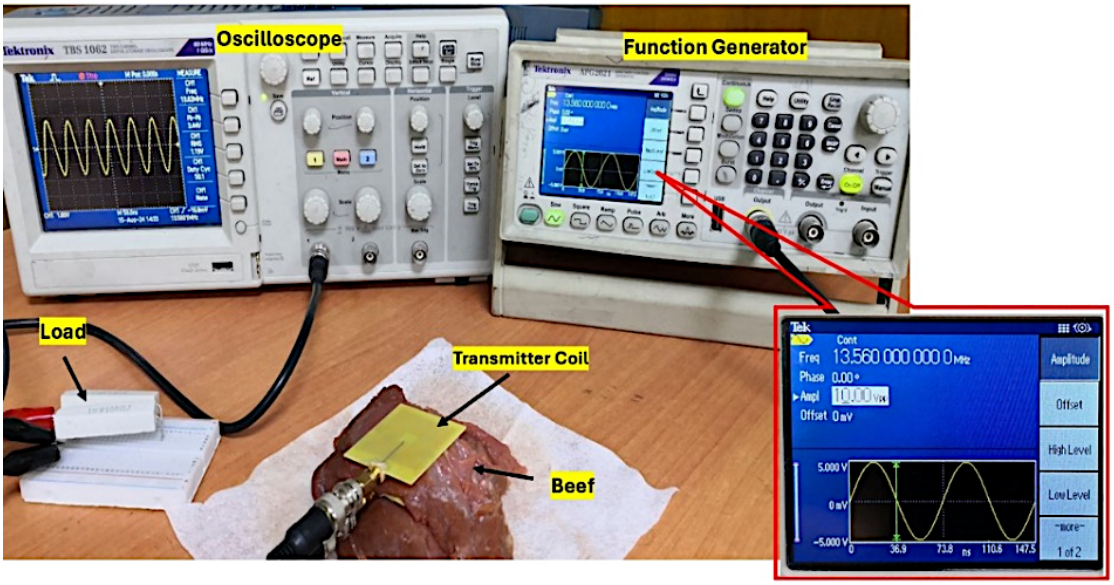

FIGURE 15. System measurement using a load resistor of 200 Ω with beef tissue.

creases, with the difference being more pronounced at shorter distances. The deviation between experimental and simulated results is minimal, with an error percentage of approximately 8%. Furthermore, this research has potential applications in implantable cardiac pacemakers.

4.4. Comparison with Previous Works

The proposed system was compared with recent related studies based on the number of layers, receiver outer diameter, frequency, transfer distance, SAR testing, medium, and efficiency (simulation or measurement). This comparison was conducted to evaluate the proposed model against existing designs and identified areas of improvement. The results of this comparison are presented in Table 4.

Increasing the number of layers enhanced the inductance and quality factor of the coils. The proposed system also reduced both the transmitter's outer diameter and implanted (receiver) outer diameter. The design operates within the ISM band frequency, aligning with related studies. Transfer distance was a critical factor in the coil design, while SAR testing was essential for high-frequency system validation. Furthermore, the medium between the transmitter and receiver coils played a crucial role in assessing system efficiency.

Efficiency measures the power delivered from the transmitter to the implanted receiver. Compared to prior studies, the proposed model demonstrated higher efficiency. Increased efficiency allows more power to be transferred from the transmitter to the implanted receiver coils, enhancing the system's

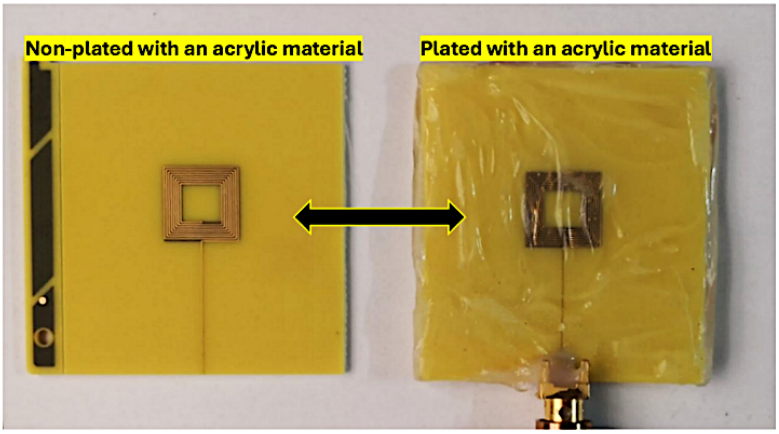

FIGURE 16. The acrylic material covers the receiver (implanted) coil.

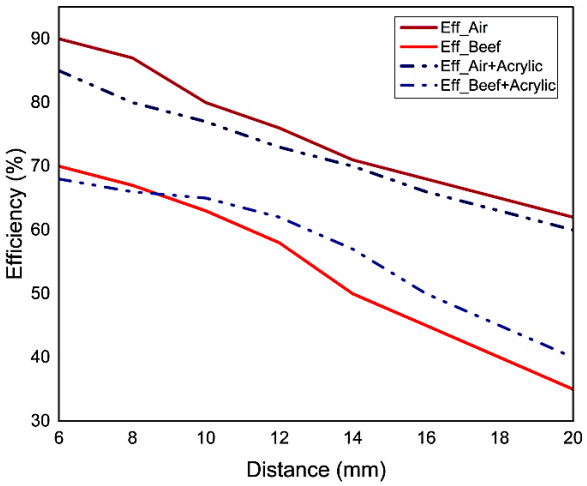

FIGURE 17. Efficiency vs. distance for measured designs at 6 to 20 mm distances with load resistance 50 Ω.

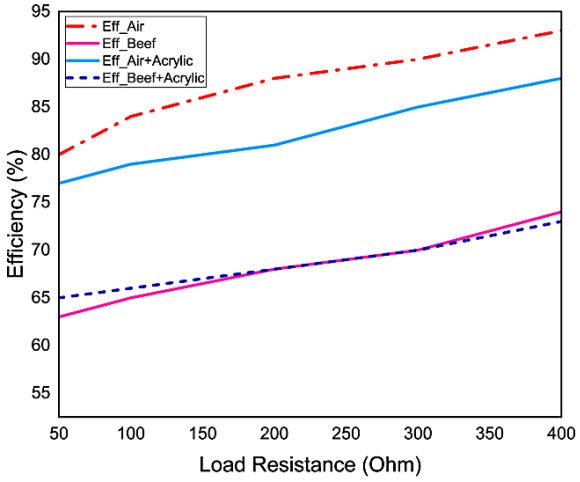

FIGURE 18. The efficiency of various load resistances across multiple mediums at a distance of 10 mm.

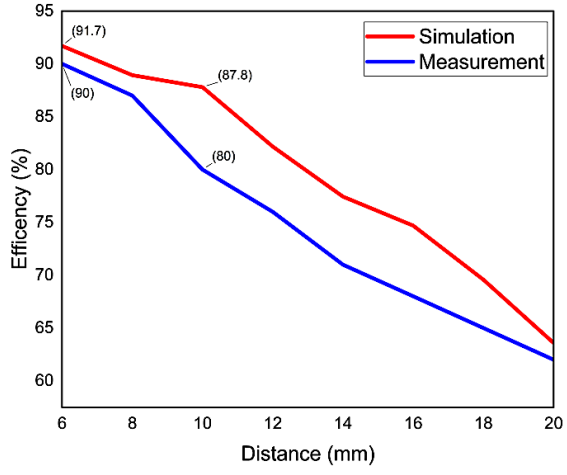

FIGURE 19. Efficiency vs. distance for simulated and measured designs at 6 to 20 mm distances with a 50 Ω load resistance.

practicality. Mehri et al. [42], Ahire et al. [15], and By Büyüktuna et al. [43] achieved high efficiency, but their implantable coil sizes were larger, and their tests were conducted only in air.

TABLE 3. Result of simulation and measurement of triple layer design at 10 mm operating distance and 13.56 MHz ISM band.

Parameters	Triple Layer Design	
	Simulation Results	Measured Results
L_1 (μH)	4.77	5.73
Q_1	116.10	97.6
R_{s1} (Ω)	3.5	5
L_2 (μH)	4.39	6.45
Q_2	153.41	91.6
R_{s2} (Ω)	2.43	6
k	0.09	0.09
M (nH)	40.9	56.36
η_{max} (%)	87.8	80

In conclusion, the proposed model performed exceptionally well in all evaluated aspects, as summarized in Table 4. The system was designed with a 10-mm implanted coil and achieved an effective 80% transfer efficiency at a 10-mm distance, demonstrating improvements in both size and efficiency com-

TABLE 4. The proposed system comparison with current investigations.

Ref./Year	No. of Layers	Receiver outer diameter (mm)	Frequency (MHz)	Transfer distance (mm)	SAR test	Medium	Efficiency (%)	
							Simulation	Measured
Na et al. [44]/2014	1	9	16.47	70	1.74 W/kg	Air Tissue		N/A
Gong et al. [45]/2017	1	20	2	8	< 2 W/kg	Tissue		59
Mehri et al. [42]/2018	3	23	13.56	10	N/A	Air		90
Erfani et al. [46]/2018	1	20	0.2-20	3	< 2 W/kg	Tissue	51.9	
N. Ha-Van and C. Seo [47]/2019	1	9	13.56	50-80	< 2 W/kg	Air Tissue		
Omran et al. [48]/2019	2	8	13.56	4	N/A	Air Tissue	77.4 70.9	51.9 44.2
Xu et al. [12]/2020	1	20	13.56	6	< 2 W/kg	Air		35
Ahire et al. [15]/2022	1	35	6.78	10	N/A	Air		85.51
Luo et al. [11]/2023	1	10	13.56	10	N/A	Air	70	70
Mohmood et al. [49]/2023	1	30	1.78	10	N/A	Air		95.75
Edanur et al. [43]/2024	1	40	13.56	N/A	< 4 W/kg	Air	96.9	
Proposed design	3	10	13.56	10	0.1823 W/kg	Air Tissue Acrylic	87. 70	80 63 65

pared to previous models. These findings suggest that the proposed approach can significantly enhance wireless power transfer for biomedical applications, offering promising prospects for the future of the field.

5. CONCLUSION

This work presents an inductive coupling system for energy transfer to implantable devices using the 13.56 MHz ISM frequency band. The primary goal is to minimize the size of the implanted coil while achieving high transfer efficiency. The proposed system consists of a single-layer transmitter coil paired with single-layer, double-layer, and triple-layer receiver coils. The system was tested using air and biological tissue as separation media between the transmitter and receiver coils. To enhance the system's performance — particularly in terms of inductance, quality factor, and efficiency — a double-layer receiver coil was designed. The final stage of the simulation involved developing a triple-layer receiver coil with a size of 10 mm, which significantly improved efficiency to approximately 87.9% due to the increased inductance of the receiving coil. The system's behavior was simulated using constitutive parameters from human biological tissue models. The receiver coil was implanted at a depth of 6 mm within body tissue, a depth suitable for interaction with nerves and muscles. Simulations indicated that the proposed design performed well in an air medium but was less efficient in a tissue medium due to the high dielectric constant and liquid content of human tissue. A specific absorption rate (SAR) simulation was conducted for the triple-layer design, and the results showed that SAR values were well below the safety limits set by US and European standards for 1 g of tissue. Additionally, the electric and magnetic flux distribution at 13.56 MHz was found to be suitable for medical applications. The triple-layer receiver coil was fabricated and experimentally tested using a vector network analyzer (VNA). The experimental results showed lower efficiency than the simulation, highlighting some practical limitations. One major limitation is that increasing the size of the receiver coil to improve energy transfer efficiency may lead to discomfort and greater interaction with physiological tissues, potentially causing health complications. Additionally, the study was conducted using beef tissue rather than live animal models, which may affect the accuracy of the system's efficiency assessment. Future research should focus on optimizing the system parameters, investigating the effects of lateral, axial, and angular misalignments between the transmitter and receiver, designing a four-layer receiver coil, enhancing system capability by integrating in-body biomedical sensors, and examining the impact of noise and electromagnetic compatibility (EMC) on system performance to ensure efficient power transfer between the transmitter and receiver coils.

ACKNOWLEDGEMENT

The authors would like to thank the University of Technology-Iraq and Al-Iraqia University for supporting this project. Additionally, the authors would like to express their gratitude to Universiti Teknikal Malaysia Melaka (UTeM) and the Ministry of Higher Education (MOHE) of Malaysia.

REFERENCES

[1] Abduljaleel, H. K., S. Mutashar, and S. K. Gharghan, "Survey of near-field wireless communication and power transfer for biomedical implants," *Engineering and Technology Journal*, Vol. 42, No. 08, 1080–1103, 2024.

[2] Barbruni, G. L., P. M. Ros, D. Demarchi, S. Carrara, and D. Ghezzi, "Miniaturised wireless power transfer systems for neurostimulation: A review," *IEEE Transactions on Biomedical Circuits and Systems*, Vol. 14, No. 6, 1160–1178, 2020.

[3] Nair, S. S., M. Muniyandi, D. S. Nagesh, C. V. Muraleedharan, R. Joseph, and S. Harikrishnan, "Charging current characteristics and effect of casing material in wireless recharging of active implantable medical devices using transcutaneous energy transfer system," *Progress In Electromagnetics Research M*, Vol. 122, 137–144, 2023.

[4] Hsu, H.-M., B. Yang, T.-L. Yang, H.-L. Cho, and N. Shinohara, "Dynamic wireless power transfer system with twin perpendicular receiver coils (invited paper)," *Progress In Electromagnetics Research*, Vol. 178, 93–101, 2023.

[5] Huang, P., L. Xu, and Y. Xie, "Biomedical applications of electromagnetic detection: A brief review," *Biosensors*, Vol. 11, No. 7, 225, 2021.

[6] Nurhayati, N., A. N. D. N. Fahmi, P. Puspitaningayu, O. Wiriawan, B. Raafi'u, F. A. Iskandarianto, A. J. A. Al-Gburi, A. Varshney, and S. Johari, "Wearable wideband textile coplanar vivaldi antenna for medical and IoT application," *Progress In Electromagnetics Research C*, Vol. 148, 145–156, 2024.

[7] Zaki, A. Z. A., E. K. I. Hamad, T. G. Abouelnaga, H. A. Elsadek, S. A. Khaleel, A. J. A. Al-Gburi, and Z. Zakaria, "Design and modeling of ultra-compact wideband implantable antenna for wireless ISM band," *Bioengineering*, Vol. 10, No. 2, 216, 2023.

[8] Yan, X., J. Yao, W. Chen, and Y. Song, "Wireless power transfer system for cardiac pacemakers based on multi-coil series magnetic integration," *Progress In Electromagnetics Research C*, Vol. 143, 87–98, 2024.

[9] Al-Gburi, A. J. A., M. M. Ismail, N. J. Mohammed, and T. A. H. Alghamdi, "SAR flexible antenna advancements: Highly conductive polymer-graphene oxide-silver nanocomposites," *Progress In Electromagnetics Research M*, Vol. 127, 23–30, 2024.

[10] Al-Gburi, A. J. A., N. H. M. Radi, T. Saeidi, N. J. Mohammed, Z. Zakaria, G. S. Das, A. Buragohain, and M. M. Ismail, "Superconductive and flexible antenna based on a tri-nanocomposite of graphene nanoplatelets, silver, and copper for wearable electronic devices," *Journal of Science: Advanced Materials and Devices*, Vol. 9, No. 3, 100773, 2024.

[11] Luo, J., R. Xue, J. Cheong, X. Zhang, and L. Yao, "Design and optimization of planar spiral coils for powering implantable neural recording microsystem," *Micromachines*, Vol. 14, No. 6, 1221, 2023.

[12] Xu, D., Q. Zhang, and X. Li, "Implantable magnetic resonance wireless power transfer system based on 3d flexible coils," *Sustainability*, Vol. 12, No. 10, 4149, 2020.

[13] Mahmood, A. I., S. K. Gharghan, M. A. A. Eldosoky, and A. M. Soliman, "Powering implanted sensors that monitor human activity using spider-web coil wireless power transfer," *IET Power Electronics*, Vol. 16, No. 8, 1339–1354, 2023.

[14] Kamarudin, S. I., A. Ismail, A. Sali, M. Y. Ahmad, I. Ismail, and K. Navaie, "5G magnetic resonance coupling planar spiral coil wireless power transfer," *Trends in Sciences*, Vol. 20, No. 1, 3444, 2023.

[15] Ahire, D. B., V. J. Gond, and J. J. Chopade, "Geometrical parameter optimization of planner square-shaped printed spiral coil for efficient wireless power transfer system to biomedical implant application," *E-Prime — Advances in Electrical Engineering, Electronics and Energy*, Vol. 2, 100045, 2022.

[16] Mahmood, M. F., S. K. Gharghan, S. L. Mohammed, A. Al-Naji, and J. Chahl, "Design of powering wireless medical sensor based on spiral-spider coils," *Designs*, Vol. 5, No. 4, 59, 2021.

[17] Zhao, W. and S. Mai, "Design of high efficiency planar spiral coil for implantable wireless power transfer systems," in *2022 IEEE International Symposium on Circuits and Systems (ISCAS)*, 147–151, Austin, TX, USA, May–Jun. 2022.

[18] Wang, J., E. G. Lim, M. P. Leach, Z. Wang, R. Pei, Z. Jiang, and Y. Huang, "A 403 MHz wireless power transfer system with tuned split-ring loops for implantable medical devices," *IEEE Transactions on Antennas and Propagation*, Vol. 70, No. 2, 1355–1366, 2022.

[19] Bao, J., S. Hu, Z. Xie, G. Hu, Y. Lu, and L. Zheng, "Optimization of the coupling coefficient of the inductive link for wireless power transfer to biomedical implants," *International Journal of Antennas and Propagation*, Vol. 2022, No. 1, 8619514, 2022.

[20] Abed, B. H., J. H. Majeed, and N. A. Habeeb, "Optimization of bio-implantable power transmission efficiency based on input impedance," *Computer Systems Science & Engineering*, Vol. 38, No. 1, 17, 2021.

[21] Ouacha, B., H. Bouyghf, N. Mohammed, and S. Abenna, "DEA-based on optimization of inductive coupling for powering implantable biomedical devices," *International Journal of Power Electronics and Drive Systems*, Vol. 13, No. 3, 1558–1567, 2022.

[22] Huh, S., B. Park, S. Choi, Y. Shin, H. Kim, J. Kim, J. Park, D. Park, and S. Ahn, "Transmitter coils selection method for wireless power transfer system with multiple transmitter coils and single receiver coil," *IEEE Transactions on Power Electronics*, Vol. 38, No. 3, 4092–4109, 2023.

[23] Jiang, C., X. Li, S. W. M. Lian, Y. Ying, J. S. Ho, and J. Ping, "Wireless technologies for energy harvesting and transmission for ambient self-powered systems," *ACS Nano*, Vol. 15, No. 6, 9328–9354, 2021.

[24] Alipour, A., A. C. Seifert, B. N. Delman, P. M. Robson, R. Shrivastava, P. R. Hof, G. Adriany, Z. A. Fayad, and P. Balchandani, "Improvement of magnetic resonance imaging using a wireless radiofrequency resonator array," *Scientific Reports*, Vol. 11, No. 1, 23034, 2021.

[25] Rong, C., C. Lu, Y. Zeng, X. Tao, X. Liu, R. Liu, X. He, and M. Liu, "A critical review of metamaterial in wireless power transfer system," *IET Power Electronics*, Vol. 14, No. 9, 1541–1559, 2021.

[26] Luo, B., T. Long, L. Guo, R. Dai, R. Mai, and Z. He, "Analysis and design of inductive and capacitive hybrid wireless power transfer system for railway application," *IEEE Transactions on Industry Applications*, Vol. 56, No. 3, 3034–3042, 2020.

[27] Liu, Z., M. Su, Q. Zhu, L. Zhao, and A. P. Hu, "A dual frequency tuning method for improved coupling tolerance of wireless power transfer system," *IEEE Transactions on Power Electronics*, Vol. 36, No. 7, 7360–7365, 2021.

[28] Maulana, E., Z. Abidin, and W. Djuriatno, "Wireless power transfer characterization based on inductive coupling method," in *2018 Electrical Power, Electronics, Communications, Controls and Informatics Seminar (EECCIS)*, 164–168, Batu, Indonesia, Oct. 2018.

[29] Mahesh, A., B. Chokkalingam, and L. Mihet-Popa, "Inductive wireless power transfer charging for electric vehicles — A review," *IEEE Access*, Vol. 9, 137 667–137 713, 2021.

[30] Sun, G., B. Muneer, Y. Li, and Q. Zhu, "Ultracompact implantable design with integrated wireless power transfer and RF transmission capabilities," *IEEE Transactions on Biomedical Circuits and Systems*, Vol. 12, No. 2, 281–291, 2018.

[31] Javan-Khoshkholgh, A., J. C. Sassoon, and A. Farajidavar, "A wireless rechargeable implantable system for monitoring and pacing the gut in small animals," in *2019 IEEE Biomedical Circuits and Systems Conference (BioCAS)*, 1–4, Nara, Japan, Oct. 2019.

[32] Zhang, K., C. Liu, Z. H. Jiang, Y. Zhang, X. Liu, H. Guo, and X. Yang, "Near-field wireless power transfer to deep-tissue implants for biomedical applications," *IEEE Transactions on Antennas and Propagation*, Vol. 68, No. 2, 1098–1106, 2020.

[33] Park, Y., S.-T. Koh, J. Lee, H. Kim, J. Choi, S. Ha, C. Kim, and M. Je, "33.7 A frequency-splitting-based wireless power and data transfer IC for neural prostheses with simultaneous 115 mW power and 2.5 Mb/s forward data delivery," in *2021 IEEE International Solid-State Circuits Conference (ISSCC)*, Vol. 64, 472–474, San Francisco, CA, USA, Feb. 2021.

[34] Wang, Q., M. A. Saket, A. Troy, and M. Ordonez, "A self-compensated planar coil for resonant wireless power transfer systems," *IEEE Transactions on Power Electronics*, Vol. 36, No. 1, 674–682, 2021.

[35] Du, X. and D. Dujic, "Modeling and design optimization of loosely coupled PCB spiral coils in inductive power transfer systems," *IEEE Transactions on Power Electronics*, Vol. 38, No. 11, 13 430–13 442, 2023.

[36] Noroozi, B. and B. I. Morshed, "Misalignment-tolerant planar spiral coil pair design for 13.56 MHz inductive coupling of wireless resistive analog passive sensors," *Sensors*, Vol. 24, No. 3, 752, 2024.

[37] Faria, A., L. Marques, C. Ferreira, F. Alves, and J. Cabral, "A fast and precise tool for multi-layer planar coil self-inductance calculation," *Sensors*, Vol. 21, No. 14, 4864, 2021.

[38] Zhao, J., "A new calculation for designing multilayer planar spiral inductors," *EDN (Electrical Design News)*, Vol. 55, No. 14, 37, 2010.

[39] Pérez-Nicoli, P., F. Silveira, and M. Ghovanloo, "Inductive link: Practical aspects," in *Inductive Links for Wireless Power Transfer: Fundamental Concepts for Designing High-Efficiency Wireless Power Transfer Links*, 53–75, Springer, 2021.

[40] Abdul-Al, M., A. S. I. Amar, I. Elfergani, R. Littlehales, N. O. Parchin, Y. Al-Yasir, C. H. See, D. Zhou, Z. Z. Abidin, M. Alibakhshikenari, *et al.*, "Wireless electromagnetic radiation assessment based on the Specific Absorption Rate (SAR): A review case study," *Electronics*, Vol. 11, No. 4, 511, 2022.

[41] Lee, A.-K., S.-E. Hong, M. Taki, K. Wake, and H. D. Choi, "Comparison of different sar limits in sam phantom for mobile phone exposure," in *2018 Asia-Pacific Microwave Conference (APMC)*, 687–689, Kyoto, Japan, Nov. 2018.

[42] Mehri, S., A. C. Ammari, J. B. H. Slama, and M. Sawan, "Design optimization of multiple-layer PSCs with minimal losses for efficient and robust inductive wireless power transfer," *IEEE Access*, Vol. 6, 31 924–31 934, 2018.

[43] Büyüktuna, E., E. Dilek, F. N. Yorgancılar, R. Çetin, and A. Ağçal, "A wireless power transfer system design for charging of intra-body implant devices," *Uludağ Üniversitesi Mühendislik Fakültesi Dergisi*, Vol. 29, No. 1, 139–154, 2024.

[44] Na, K., H. Jang, H. Ma, and F. Bien, "Tracking optimal efficiency of magnetic resonance wireless power transfer system for biomedical capsule endoscopy," *IEEE Transactions on Microwave Theory and Techniques*, Vol. 63, No. 1, 295–304, 2014.

[45] Gong, C., D. Liu, Z. Miao, and M. Li, "A magnetic-balanced inductive link for the simultaneous uplink data and power telemetry," *Sensors*, Vol. 17, No. 8, 1768, 2017.

[46] Erfani, R., F. Marefat, and P. Mohseni, "Biosafety considerations of a capacitive link for wireless power transfer to biomedical implants," in *2018 IEEE Biomedical Circuits and Systems Conference (BioCAS)*, 1–4, Cleveland, OH, USA, Oct. 2018.

[47] Ha-Van, N. and C. Seo, "Modeling and experimental validation of a butterfly-shaped wireless power transfer in biomedical implants," *IEEE Access*, Vol. 7, 107 225–107 233, 2019.

[48] Omran, M. M., S. Mutashar, and A. Ezzulddin, "Design of an $(8 \times 8)\,\mathrm{mm}^2$ efficient inductive power link for medical applications," in *2019 2nd International Conference on Engineering Technology and its Applications (IICETA)*, 61–66, Al-Najef, Iraq, Aug. 2019.

[49] Mahmood, A. I., S. K. Gharghan, M. A. Eldosoky, and A. M. Soliman, "Wireless charging for cardiac pacemakers based on class-D power amplifier and a series–parallel spider-web coil," *International Journal of Circuit Theory and Applications*, Vol. 51, No. 1, 1–17, 2023.